JOURNAL OF GEOPHYSICAL RESEARCH, VOL. 105, NO. D1, PAGES 1585–1597, JANUARY 20, 2000

Influence of valley winds on transport and dispersion of airborne pollutants in the Freiburg-Schauinsland area

N. Kalthoff, V. Horlacher, and U. Corsmeier
Institut für Meteorologie und Klimaforschung, Forschungszentrum Karlsruhe/Universität Karlsruhe
Karlsruhe, Germany

A. Volz-Thomas, B. Kolahgar, and H. Geiß
Institut für Chemie der belasteten Atmosphäre, Forschungszentrum Jülich, Jülich, Germany

M. Möllmann-Coers and A. Knaps
Abteilung Sicherheit und Strahlenschutz, Forschungszentrum Jülich, Julich, Germany

Abstract. The change of the concentration of trace gases in a natural environment depends on both chemical and meteorological conditions. To quantify the contribution of meteorological processes, such as transport and dispersion, chemical and meteorological processes must be assessed separately. In June 1996 the Schauinsland Ozone Precursor Experiment (SLOPE) was carried out to investigate the behavior of ozone and its precursors as a function of time in a valley between Freiburg in the Rhine Valley and Schauinsland in the Black Forest [*Volz-Thomas et al.*, this issue]. The main purpose of this contribution is to calculate the influence of transport and dispersion on the change of the concentration of airborne pollutants in a propagating air mass. Therefore (1) an inert tracer, SF_6, was released, and (2) meteorological measurements were performed to investigate the valley wind regimes and the evolution of the mixed layer. Here are the main results of the experiment: Clear-sky conditions caused upvalley winds to be generated in the various valleys in the morning. These upvalley winds led to the transport of polluted air and SF_6 from Freiburg through the Zarten Basin and the side valley (Großes Tal) up to the Schauinsland hill. The propagation through the Großes Tal took 90 ± 5 min, which gives a propagation rate of approximately 1.3 m s^{-1}. The dilution factor for SF_6 between the entrance and the outlet of the valley was approximately 9. This dilution factor could not only be explained by the continuous growth of the boundary layer during the propagation time of the tracer from the entrance to the outlet of the valley, but additionally by flow splitting and mountain venting [*Fiedler et al.*, this issue].

1. Introduction

Regions with complex terrain or with markedly different surface properties are frequently characterized by diurnal cyclic wind systems, such as mountain, valley, and slope winds [*Atkinson*, 1981; *Whiteman*, 1990; *Barry*, 1992]. The changes from day to night regimes depend on such factors as sunrise and sunset, the orientation of the axis of a valley, and the size of the valley. All this makes the wind field at ground level over complex terrain a very complex structure, which is superimposed upon the larger-scale synoptic wind field. High wind shear consequently arises at the upper boundary of these regional wind systems. These wind systems are very important in connection with airborne pollutant transport processes. In light of this aspect, it is understandable that a large number of experiments and studies have already been conducted in order to improve our knowledge of the development, as a function of time, and the geographic extension of valley wind systems in valleys of different sizes [e.g., *Steinacker*, 1984; *Hennemuth*, 1986; *Freytag*, 1987; *Vergeiner and Dreiseitl*, 1987; *Freytag*, 1988].

Orographically complex terrain is not only characterized by the complex structure of the wind fields it causes, but frequently also by variations in space of the heights of the boundary layer or mixed layer [e.g., *de Wekker*, 1995; *Kalthoff et al.*, 1998; *Koßmann et al.*, 1998]. In most cases the height of the mixed layer is coupled to the height of the valley wind system [*Ye et al.*, 1987; *Segal et al.*, 1988]. The height of the mixed layer regulates vertical mixing, and its variation in space in many cases also contributes to a more thorough exchange of air masses between the boundary layer and the free atmosphere [*Allwine*, 1993] than is the case over homogeneous surfaces. These air masses are then available for long-distance transport in the free atmosphere. In many cases, cities with industries are located at the bottom of slopes or in the transition area from flatlands to hilly terrain or at the exits of valleys. As a consequence, both meteorological phenomena, the regional wind system and the height of the mixed layer varying as a function of space, are important in the ventilation and human and biometeorological conditions of such regions [*Carroll and Baskett*, 1979; *Wakimoto and McElroy*, 1986; *Kurita et al.*, 1990; *Vögtlin et al.*, 1997; *Bischoff-Gauß et al.*, 1998]. The influence of secondary circulation systems upon pollutant transport was therefore studied in detail in field experiments, such as ASCOT [*Clements et al.*, 1989].

Airborne pollutants in transit do not only undergo diffusion

Paper number 1999JD900999.
0148-0227/00/1999JD900999$09.00

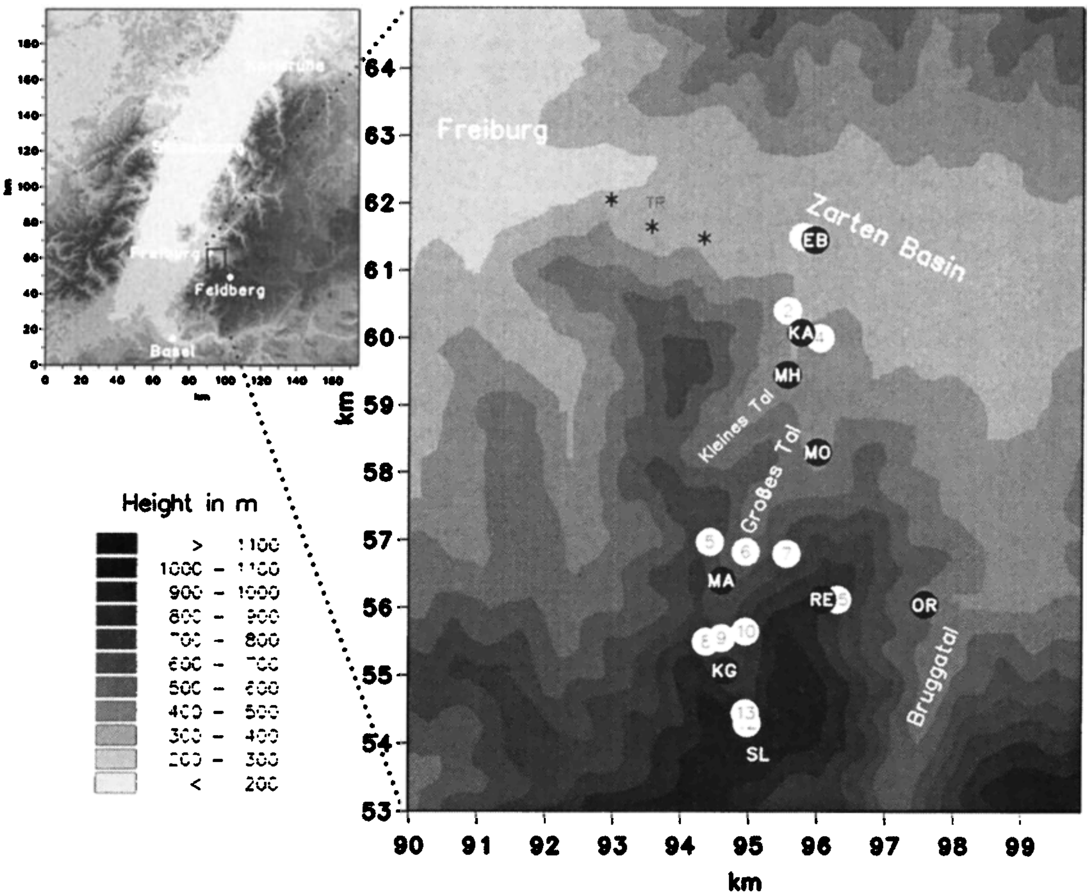

Figure 1. Experimental area in the Black Forest near Freiburg in south Germany: Tracer release (TR) sites; tracer monitoring sites indicated by numbers 1 to 15; and surface and upper air sounding stations for meteorological parameters Ebnet (EB), Kappel (KA), Maierhof (MH), Molzhof (MO), Marxenhof (MA), Kohlengrund (KG), Schauinsland (SL), Rappeneck (RE), and Oberried (OR).

but also chemical transformations and deposition. To assess whether chemical conversion processes are interpreted correctly under the prevailing environmental conditions, the contributions made by transport and diffusion must be separated from those of chemical transformation. One way of achieving this is by using an inert tracer, as all changes in tracer concentration are due to transport and diffusion exclusively. A large number of experiments with tracers were conducted in the past, but mainly to study the complex wind field structure in valleys and the associated airborne pollutant transport in valleys [*Wilson et al.*, 1983; *Gudiksen et al.*, 1984; *King et al.*, 1987; *Orgill*, 1989; *Whiteman*, 1989; *Allwine*, 1993].

The problem referred to above, that is, pollutant transport from urban regions into mountainous regions during the day, and the supply of low-pollutant air from mountainous regions into urban regions during the night, which is associated with diurnal cyclic wind systems, has been known for a long time to exist in the Freiburg region [*Loßnitzer*, 1942; *Rudloff*, 1980; *Groß*, 1989]. To exploit this existing knowledge, the Schauinsland Ozone Precursor Experiment (SLOPE) was conducted in this region in the summer of 1996 to investigate the transport, diffusion, and photochemical formation of ozone and the degradation of the precursors in the city plume of Freiburg on its way to the Schauinsland, a hill of the Black Forest [*Volz-Thomas et al.*, this issue]. Freiburg in the Rhine Valley is located at the exit of the Zarten Basin, from where various valleys branch off into the Black Forest (Figure 1). After the onset of the valley winds, pollutants are expected to be transported from Freiburg via the Zarten Basin and the Großes Tal to the Schauinsland. The measurements took place in the Großes Tal, a valley which branches off the Zarten Basin toward the south and ends at the Schauinsland mountain. The experiment included chemical [*Pätz et al.*, this issue; B. Kolahgar et al., unpublished manuscript, 1999], meteorological, and tracer measurements. The problems to be solved by the meteorological observations and the tracer experiment included the following: (1) What is the transport time of the tracer between the entrance and the outlet of the Großes Tal? This quantity is needed for the calculation of chemical transformation processes. (2) What is the dilution factor of the tracer between the entrance and the outlet of the Großes Tal? This information is necessary to separate the dilution from the chemical transformation processes [*Volz-Thomas and Kolahgar*, this issue]. (3) What is the onset and offset of the valley wind systems in the Großes Tal and the Zarten Basin? With these data the decision can be made as to which period can be applied for the calculation of the dilution factor. (4) What is the vertical evolution of the mixed layer height during that period? That is, can the dilution of the tracer be explained by the increase of the mixed layer? The questions raised here are the subject of this contribution. Additionally, calculations with the three-dimensional Karlsruhe Atmospheric Mesoscale Model (KAMM) were performed to provide interpretation aids for the analysis of the tracer concentrations and the meteorological phenomena observed [*Fiedler et al.*, this issue].

The paper is arranged as follows: The experimental layout section (section 2) contains an overview of the meteorological measurements, the tracer release and the sampling network, and of the meteorological conditions on June 5, 1996, 1 day in one of the two intense measuring periods. Section 3 describes the diurnal cycle of the valley wind systems and the vertical growth of the upvalley wind system and the mixed-layer depth. Finally, in section 4 the dilution of the tracer between the entrance and the outlet of the valley is discussed and compared with the dilution expected from mixed-layer growth.

2. Meteorological Measurements, Tracer Experiment, and Synoptic Conditions

2.1. Geography

Freiburg is located on the eastern edge of the Rhine Valley at the entrance of the Zarten Basin at an elevation of approximately 250 m mean sea level (msl). The Zarten Basin is oriented approximately from west to east and has a length of approximately 12 km and a maximum width of 3.5 km (Figure 1). Several side valleys drain into the Zarten Basin from the south, like the Großes Tal and the Bruggatal. The Großes Tal ends at the Schauinsland hill which has an elevation of 1284 m msl. The Großes Tal is approximately 8 km long and more than 1 km wide at the entrance, but very steep and narrow (500 m) at the end. There is only one road in the valley connecting a number of small settlements. Vegetation within the Zarten Basin and its side valleys is dominated by meadows, while most slopes and mountains are covered with coniferous forests.

2.2. Tracer Release and Monitoring Sites

SF_6 was used as an atmospheric tracer in this investigation. The substance is nontoxic [*Wilson et al.*, 1983; *Möllmann-Coers and Heinemann*, 1997] and can be measured in low concentrations. The tracer was released at the three sites in the Zarten Basin marked TR (Figure 1). These sites were selected from precalculations with a mesoscale model KAMM so that the tracer could be expected to be mixed over the whole valley when entering the entrance of the Großes Tal. The tracer was released approximately 4 m above ground level. Tracer data were collected in the Zarten Basin (site 1) and the Großes Tal side valley (sites 2 to 13). To investigate the homogeneity of tracer concentration, several cross sections were distributed normally to the axis of the Großes Tal (Figure 1). Additionally, one monitoring station was established below the ridgetop of two side valleys (Rappeneck, site 15) in order to study the transport of air masses by slope winds out of the valley. One sampling site was located on the Schauinsland hill (site 14). The sampling time for each of the samplers was 30 min. The sampling at the different sites started with the expected arrival of the plume. The tracer was released simultaneously at each of the three sites, TR, at a rate of 1.9 g s^{-1} between 0900 and 1030 central European time (CET) on June 5, 1996.

2.3. Meteorological and Air Quality Monitoring Sites

Surface data were monitored at seven different sites located in the Zarten Basin at Ebnet (EB), 327 m msl; in the Großes Tal at Kappel (KA), 354 m msl; Marxenhof (MA), 630 m msl; Kohlengrund (KG), 810 m msl; and on the Schauinsland (SL), 1284 m msl; on the mountain ridge at Rappeneck (RE), about

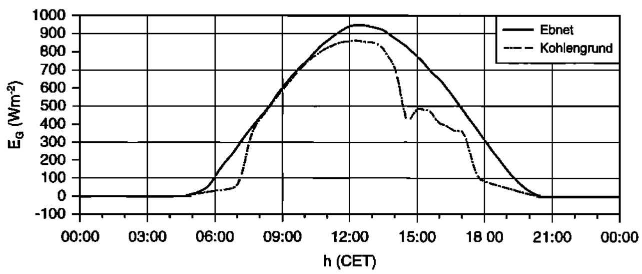

Figure 2. Global radiation E_G at Ebnet (EB) and Kohlengrund (KG) for June 5, 1996.

1000 m msl, and on a slope within the Bruggatal at Oberried (OR), 575 m msl (Figure 1). At these stations, wind speed and wind direction were measured at least at one height, while the temperature and humidity were mainly collected at two heights. In addition, a few stations (Ebnet, Oberried) collected data on the air pressure and the components of the energy balance on the surface (net radiation, sensible heat flux, latent heat flux, soil heat flux). The data were aggregated into 10-min mean values. Ambient concentrations of chemical species were measured at various sites of the Zarten Basin and the Großes Tal [*Pätz et al.*, this issue]. Results from these investigations were presented by *Volz-Thomas et al.* [this issue] and *Volz-Thomas and Kolahgar* [this issue].

Upper air soundings of meteorological parameters were performed with a radiotheodolite system in the Zarten Basin (Ebnet), tethered balloons (Maierhof, 385 m msl (MH), Molzhof 450 m msl (MO), Kohlengrund) and sodars (Kappel, Kohlengrund) in the Großes Tal. On June 5, 1996, radiosonde and tethersonde ascents were performed between 0600 and 1800 CET at intervals of approximately 1.5 hours. The wind speed and wind direction data from the sodars were integrated over 30 min.

2.4. Synoptic Conditions

The synoptic conditions on June 5, 1996, were dominated by a high-pressure system over East Germany. Southeasterly geostrophic winds were found in the measuring area with speeds of $v_g \approx 5$ m s^{-1}. In most parts of the measuring area the sky was cloud-free. Only at the mountain sites were 1/8 to 2/8 of the sky covered with cumulus clouds in the late afternoon, as is also evidenced by the lower values of global radiation E_G, shown in Figure 2. Especially for Kohlengrund, the development of cumulus clouds and strong shading by the slopes resulted in the reduction of radiation. The astronomic data for sunrise were 0451 CET and for sunset were 2013 CET.

3. Development of the Valley Wind System as a Function of Time and Space

3.1. Surface Wind Field

Three characteristic periods can be distinguished for the surface wind field. In order to appreciate more fully these "typical" periods the speed and direction of the wind were averaged over the corresponding intervals of near steady state conditions. In this way, specific key events can be pinpointed more easily on the wind field chart.

3.1.1. First period: Nighttime regime. The nighttime flow pattern is shown in Figure 3. The surface wind data were integrated from 0000 to 0400 CET. Mountain winds could be

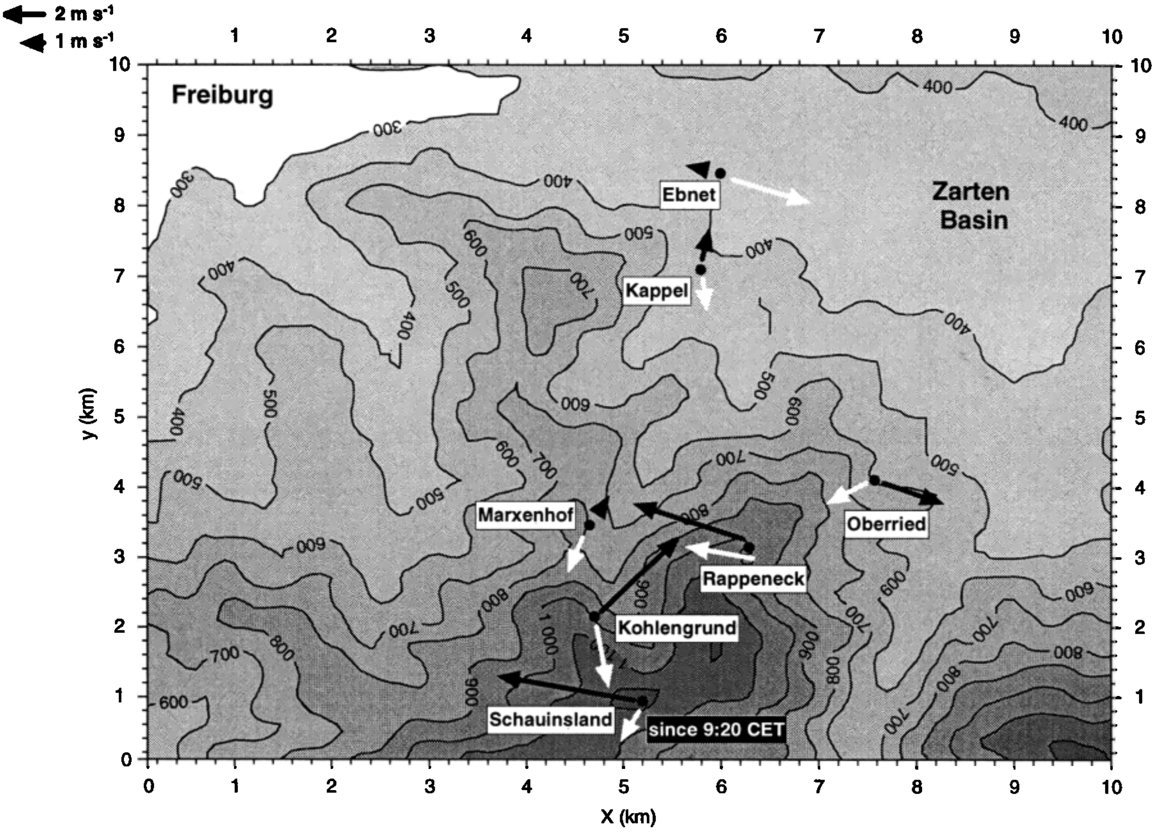

Figure 3. Flow pattern in the Freiburg-Schauinsland area between 0000 and 0400 CET (black arrows) and between 0900 and 1200 CET (white arrows) on June 5, 1996.

identified at all stations within the Großes Tal and in the Zarten Basin, while strong southeasterly winds of 5 to 6 m s^{-1} could be observed at the elevated hill sites of Schauinsland and Rappeneck. This wind direction roughly agreed with the synoptic flow conditions. At Oberried, the station situated on the slope in the Bruggatal, downslope winds were measured.

3.1.2. Morning transition regime. The timing of the changes in wind direction from downvalley winds to fully reversed upvalley winds in the Großes Tal exhibits a complex feature. As is shown in Figure 4, upvalley winds were observed first at a single site (Marxenhof) at 0500 CET. This station lies on the western slope of the Großes Tal. The change in wind direction was correlated with an increase in temperature and wind speed to levels of approximately 1 m s^{-1}. The change in wind direction occurred at about the astronomic time for sunrise, 0451 CET. However, no convincing explanation of this early change in wind direction was found. At the other stations within the Großes Tal, the transition from southerly downvalley to northerly upvalley winds started at Kappel at 0730 CET. At Kohlengrund it could be established at 0800 CET. At Schauinsland the upvalley wind arrived at 0920 CET. At that time the wind direction turned from easterly to northeasterly. In the other side valley (Bruggatal) at Oberried, the downslope regime disappeared at 0600 CET, and it took 3 hours for a fully reversed upslope flow to be established (not shown). In the Zarten Basin, transition from the nighttime to the daytime regime started at 0900 CET (Figure 5). Here the upvalley wind system was correlated with an increase in wind speed from less than 1 m s^{-1} to approximately 4 m s^{-1}. Associated with the onset of upvalley winds, also a small decrease of temperature and humidity was observed. In section 3.2 it will be demonstrated that this temperature decrease appeared throughout the whole layer of the upvalley wind regime and resulted in the evolution of a low mixing layer height.

In conclusion, it can be stated that the nighttime regime was resolved on the local scale at about sunrise. The upvalley winds, first established in the small side valleys of the Zarten Basin, propagated from the entrance upward to the end of the valley some 1½ hours after sunrise. Upvalley winds in the large Zarten Basin evolved about 3 hours after sunrise, that is, approximately 1½ hours later than the upvalley winds in the small valleys.

3.1.3. Second period: Upvalley and upslope regimes. Figure 3 also includes the surface wind pattern for the period from 0900 to 1200 CET. Thus upvalley winds in the Großes Tal and upslope winds at Oberried in the Bruggatal could be found during this interval. Wind speed reached its maximum in the Zarten Basin. At Ebnet, levels of more than 4 m s^{-1} could be found (Figure 5). At Rappeneck on the ridgetop, easterly winds still prevailed at that time (Figure 4), representing the large-scale flow.

3.1.4. Third period: Regional-scale flow. The fully established valley wind systems were disturbed at about 1200 CET. Westerly winds arose at Schauinsland and Rappeneck (Figure 4), thus reducing wind speed and changing wind direction at all sites within the Großes Tal, for example, at Kappel, Marxenhof, and Kohlengrund (Figure 4). In the Zarten Basin, only a slight increase in wind speed could be recognized between 1100 and 1200 CET (Figure 5). This is because the evolving westerly wind already corresponded to the upvalley flow in the

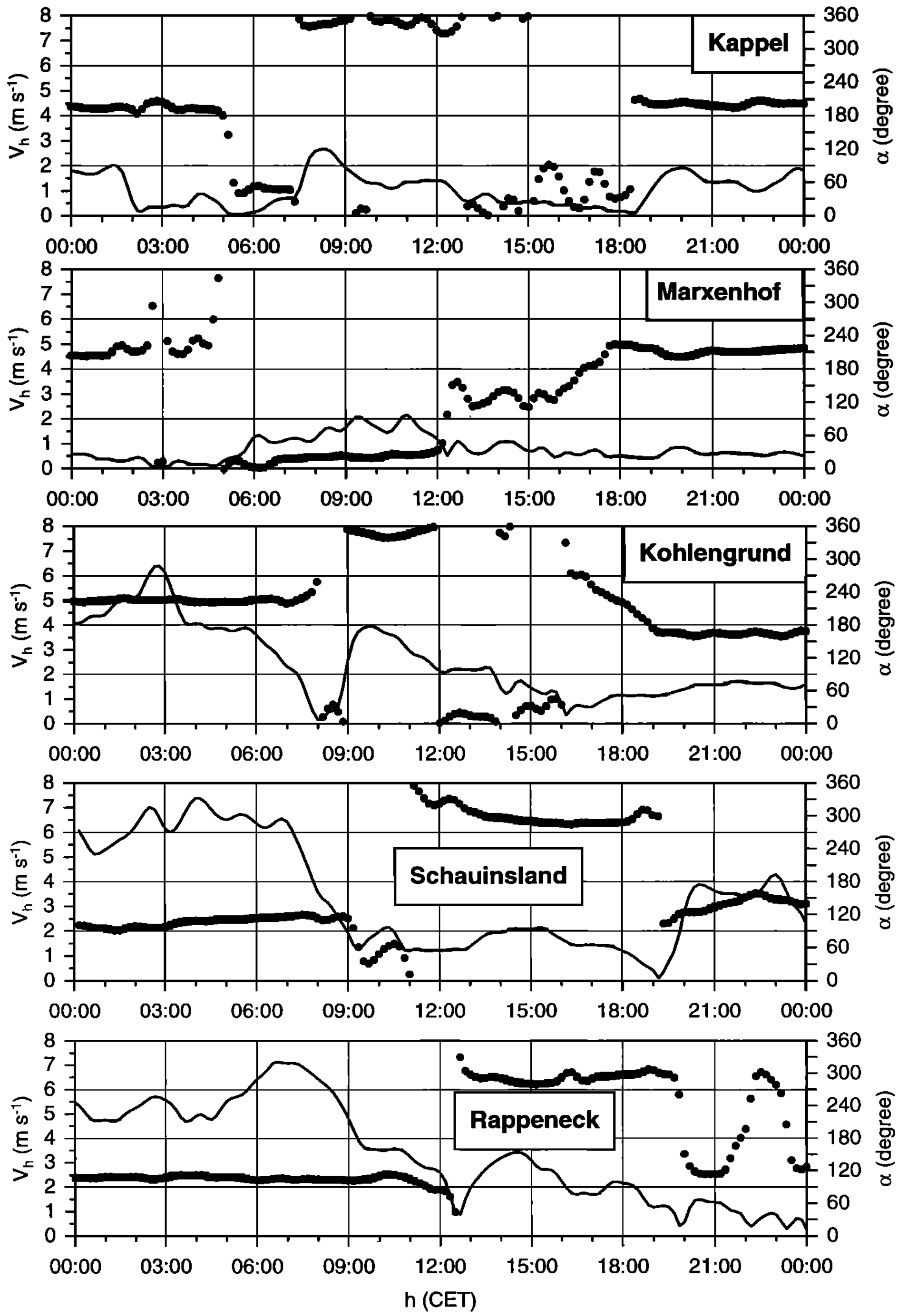

Figure 4. Wind speed v_h (solid line) and wind direction α (dots) at Kappel, Marxenhof, Kohlengrund, Schauinsland, and Rappeneck on June 5, 1996.

Zarten Basin. The westerly winds at the elevated levels of Schauinsland and Rappeneck lasted until 1800 CET. The reason for the evolution of the westerly winds can be found from model simulations performed for this particular day [*Fiedler et al.*, this issue]. Northwesterly winds developed on the Black Forest slopes of the Rhine Valley in the morning. In the course of the morning, these upslope winds reached the edge of the Black Forest slopes and penetrated farther into the Black Forest. At noon these northwesterly winds arrived at the Black Forest summits and replaced the local winds. It can therefore be concluded that only the period between 0900 and 1200 CET can be used for the calculation of the dilution factor between the entrance of the Großes Tal and the Schauinsland because after midday the transport path at Schauinsland is changed considerably.

3.1.5. Evening/nighttime regimes. The transition to the evening or nighttime regimes in the Großes Tal occurred approximately between 1800 and 1900 CET (Figure 4). The transition from upvalley winds to downvalley winds in the Zarten Basin took place between 1900 and 2000 CET (Figure 5). Thus a delay between the evolution of the downvalley wind regime in the small and the large valleys could be found again. At the

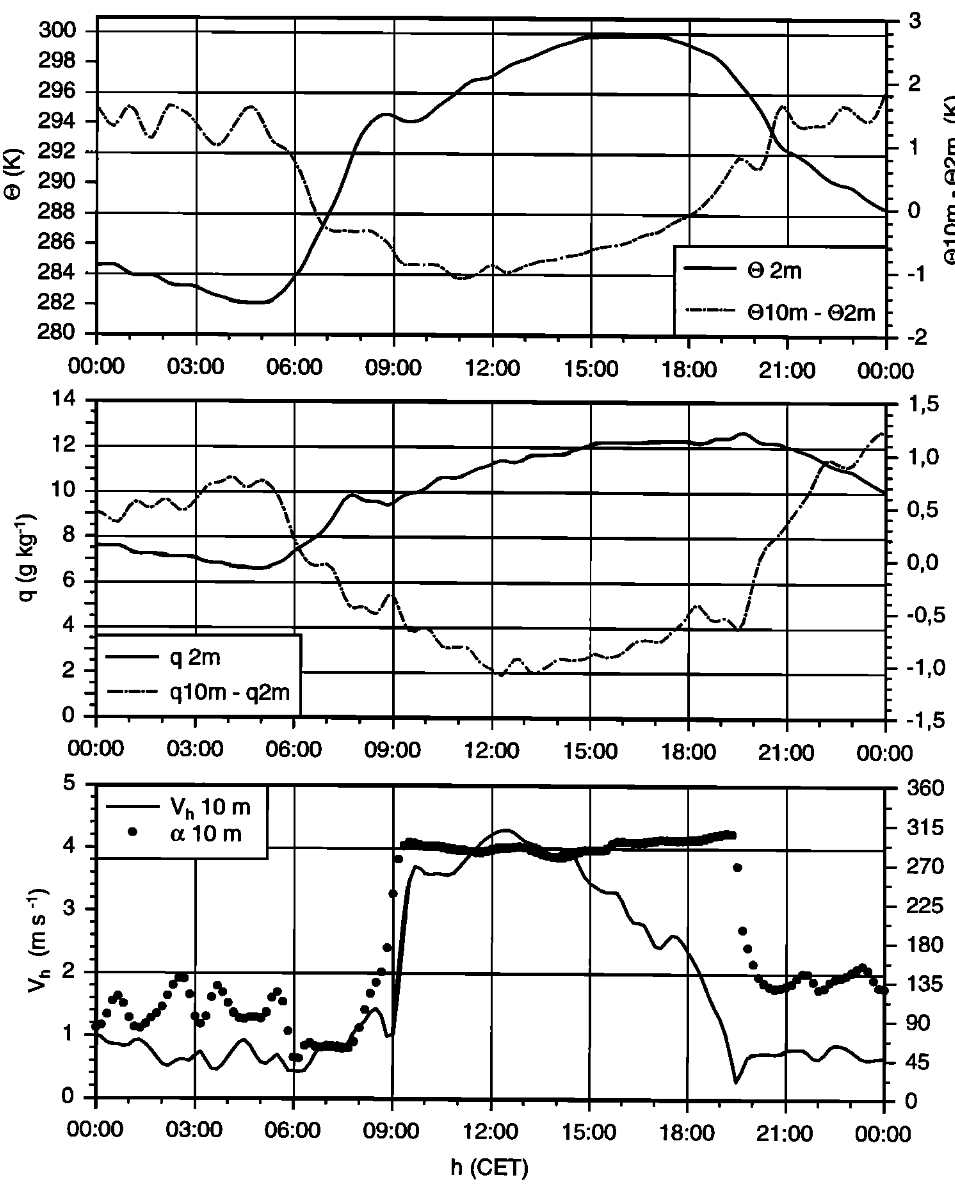

Figure 5. Potential temperature Θ, difference temperature ΔΘ, specific humidity q, humidity difference Δq, wind speed v_h, and wind direction α at Ebnet on June 5, 1996.

elevated sites of Schauinsland and Rappeneck the regional-scale westerly winds subsided between 1900 and 2000 CET, and large-scale easterly winds prevailed (Figure 4).

3.2. Vertical Growth of the Mixed-Layer Depth and Valley Wind System

3.2.1. Mixed-layer depth and valley wind system in the Großes Tal. For a simultaneous view of the mixed-layer depth and the depth of the valley wind systems, the profile data from various stations were interpolated in time. Wind vectors are presented on a cross section from south to north along the axis from the Schauinsland through the Großes Tal to Ebnet in the Zarten Basin. The mixing layer depth was determined from the temperature and humidity profiles. The wind vectors and mixing layer height for 0900 CET are shown in Figure 6. As indicated in section 3.1, upvalley winds were established in both the Großes Tal and the Zarten Basin at that time. The top of the upvalley wind is indicated in the Großes Tal by a veering of the wind direction from a northerly to southeasterly flow and a veering from a northwesterly to southeasterly flow in the Zarten Basin. The depth of the upvalley wind system in the Großes Tal ranged from 115 m at Maierhof to 240 m at Kohlengrund. At Ebnet a depth of the upvalley wind system of 170 m was detected. These heights of the upvalley winds are in agreement with the top of the mixed layer at all sites, indicated by the temperature profiles. Figures 6 also shows the profile for 1200 CET. By 1200 CET the depth of the upvalley wind system had reached levels of 370 m at Ebnet, 445 m at Maierhof, 405 m at Molzhof, and 385 m at Kohlengrund. Again, at this time, the top of the valley wind system coincided with the top of the mixed layer, a finding already modeled by *Ye et al.* [1987] and *Segal et al.* [1988]. As the maximum elevation of the tethered balloon at Kohlengrund at 1200 CET was below the top of the mixed layer, additional information from a research aircraft [*Neininger*, 1996] was used to determine the top of the

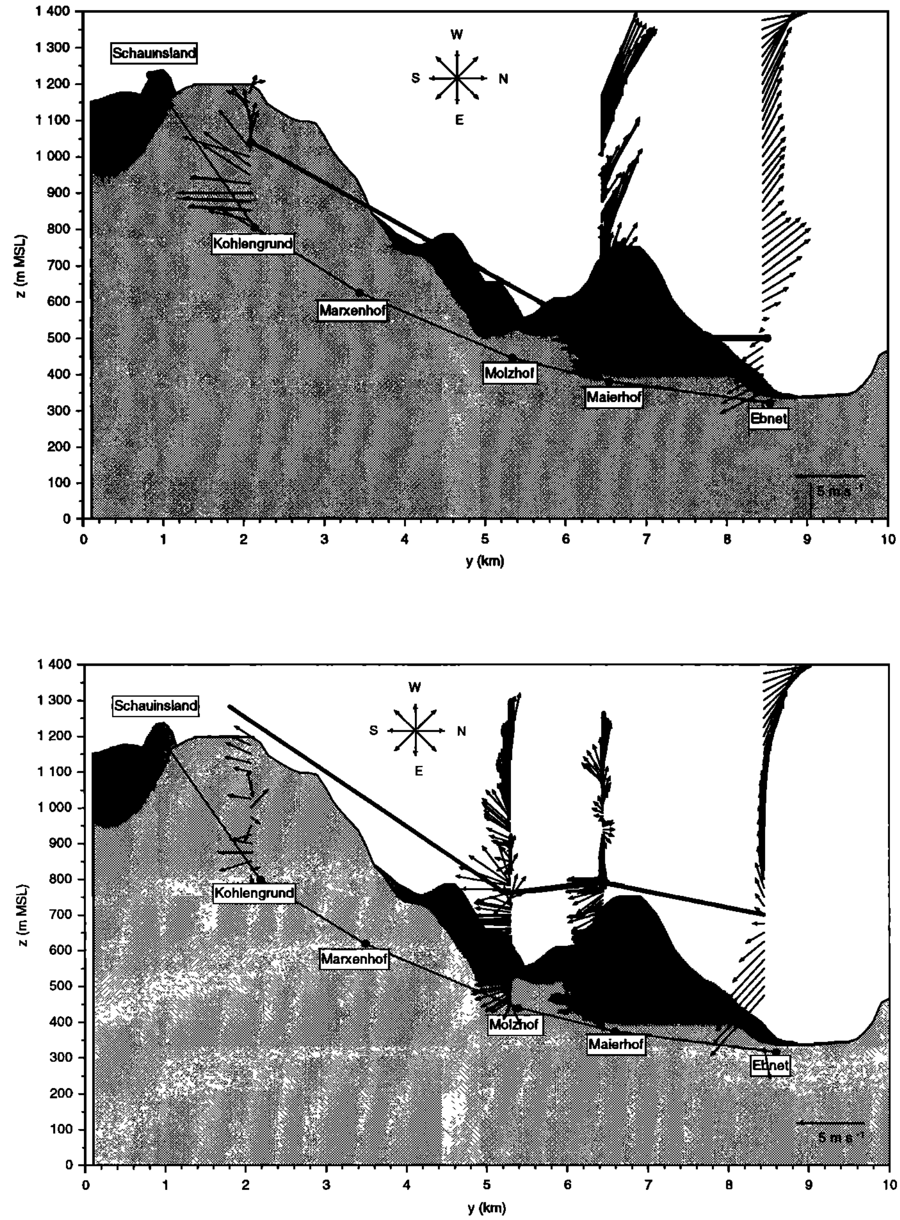

Figure 6. Cross sections through the region extending between Schauinsland in the south through the Großes Tal to Ebnet in the Zarten Basin at (top) 0900 and (bottom) 1200 CET on June 5, 1996. The light and dark grey colors mark silhouettes of the mountain ridges east and west of the Großes Tal, respectively. Areas in moderate grey indicate elevations inside the Großes Tal. The thin solid line indicates the valley ground, and the thick solid line marks the top of the mixed layer. The arrows indicate the wind vector.

mixed layer. After 1200 CET, the influence of the regional-scale westerly flow (Figure 4) led to the disturbance of the upvalley winds in the Großes Tal at elevated layers. The results of the evolution of the mixed-layer depth with time will be used in section 4 to see whether the mixed layer growth can be used to explain the decrease of the tracer between the entrance into the Großes Tal at Kappel and the outlet at Schauinsland.

3.2.2. Evolution of the valley wind system and mixing layer depth in the Zarten Basin. The initiation of the upvalley flow and the onset of convective boundary layer growth in the Zarten Basin correlated with a decrease of temperature and humidity (Figure 5). For this area a similar temperature decrease correlated with the onset of the upvalley wind had already been described by *Loßnitzer* [1942]. It is obvious from Figure 7 that this temperature decrease at approximately 0900 CET applied to the whole layer of the upvalley wind regime. At the top of the upvalley wind regime an inversion developed with an intensity of approximately 1.5 K. The onset of the upvalley flow thus did not only lead to the transport of polluted air, for example, NO_x, from Freiburg to the Zarten Basin (Figure 8) but, at the same time, caused the evolution of a low-level inversion (500 m msl). This low inversion height suppressed the effective vertical mixing of air pollutants and of the tracer. As the temperature above the upvalley wind layer rose during the morning hours to 0.7 K h^{-1}, as was calculated from the temperature profiles between 0720 and 0906 CET,

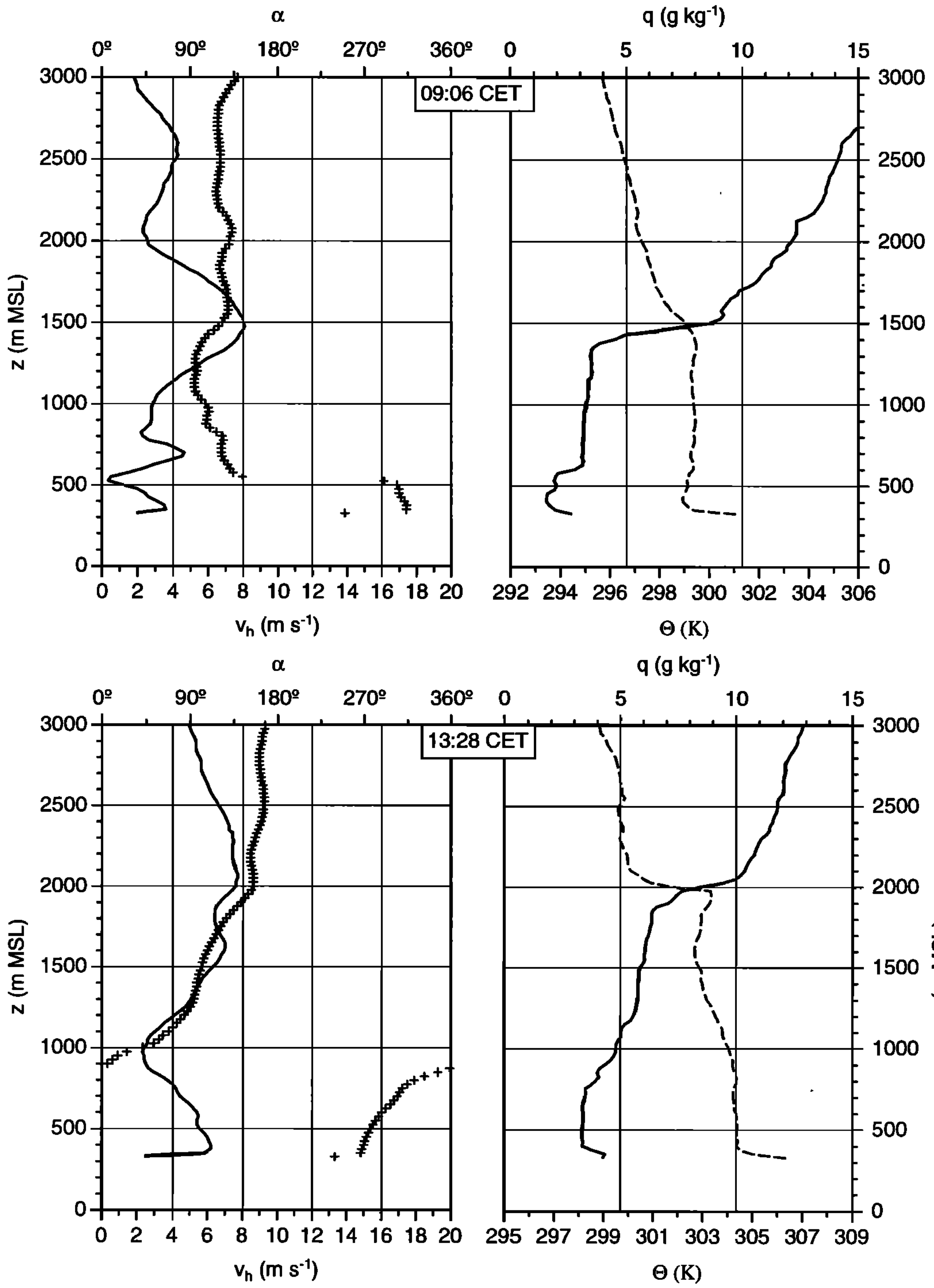

Figure 7. Profiles of wind speed v_h (solid line), wind direction α (crosses), potential temperature Θ (solid line), and specific humidity q (dashed line) at Ebnet 0906 and 1328 CET on June 5, 1996.

the erosion of this low-level inversion by the sensible heat flux took several hours. Even at 1328 CET the mixing layer depth was only 470 m, which is much lower than expected for this region under clear-air conditions in summer [*Kalthoff et al.*, 1998].

The energy budget equation [*Kraus*, 1970] can be used to obtain an insight into the processes involved in this phenomenon, especially warming of the layers above the inversion:

$$\frac{\partial \Theta}{\partial t} = -u\frac{\partial \Theta}{\partial x} - v\frac{\partial \Theta}{\partial y} - w\frac{\partial \Theta}{\partial z} - \frac{1}{\rho c_p}\left(\frac{\partial H}{\partial z} + \frac{\partial Q}{\partial z}\right), \quad (1)$$

where u, v, and w are the components of the wind vector; Q denotes the net radiation; H is the sensible heat flux; ρ is the air density; and c_p is the specific heat at constant pressure. Neglecting heating by the divergence of radiation and by the vertical advection term, local heating results

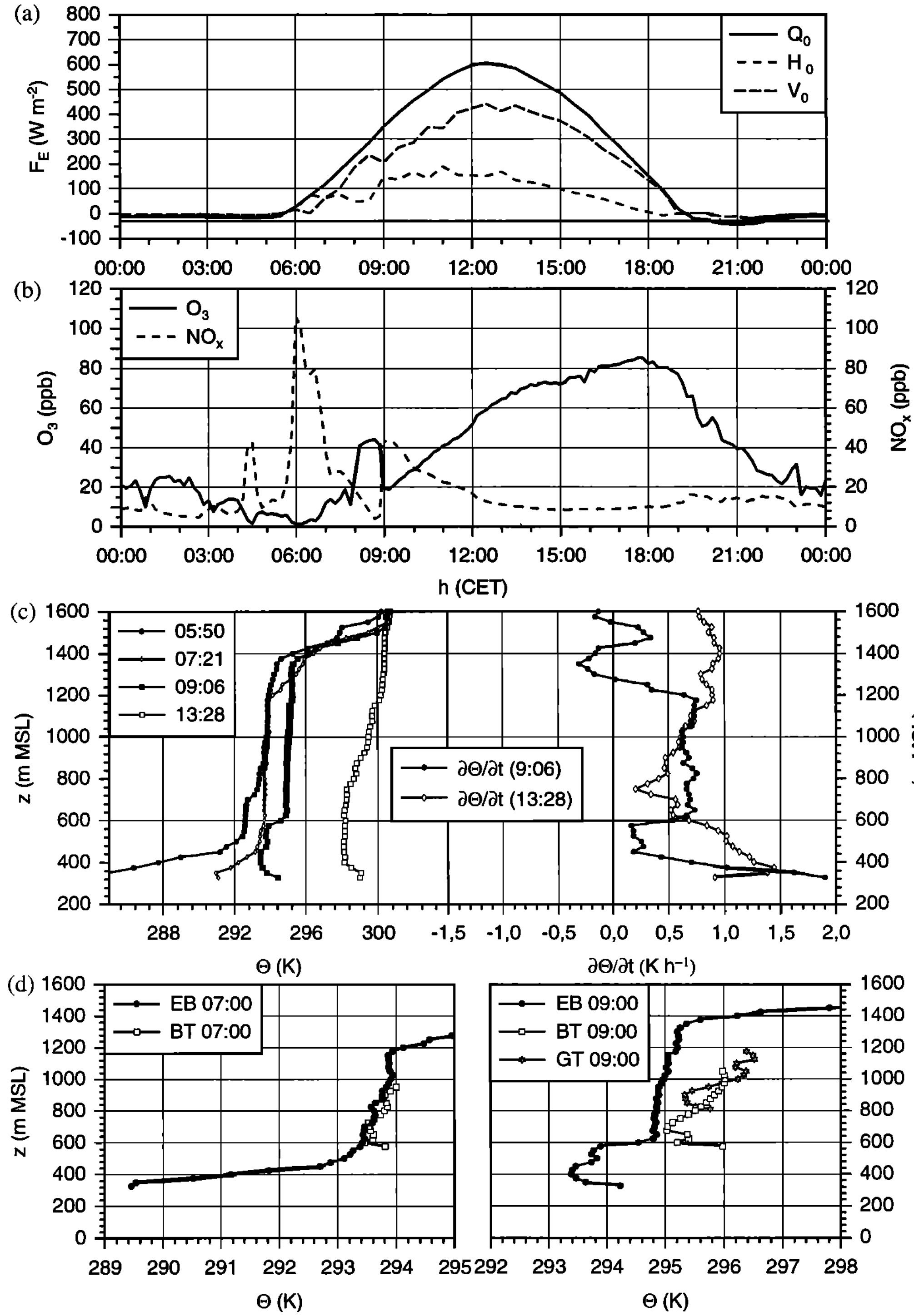

Figure 8. (a) Net radiation Q_0, sensible heat flux H_0, and latent heat flux V_0 at Ebnet on June 5, 1996. (b) O_3 and NO_x at Ebnet on June 5, 1996. (c) Profiles of potential temperature Θ and temporal derivation of the potential temperature at Ebnet at different times. (d) Profiles of potential temperature at 0700 CET on June 5, 1996, at Ebnet (EB) and Bruggatal (BT) and at 0900 CET at Ebnet (EB), Bruggatal (BT), and Großes Tal (GT).

from horizontal advection and the divergence of the sensible heat flux. The vertical advection term is assumed to be small as the upper level inversion at approximately 1400 m msl is nearly persistent in time (Figure 8); that is, no subsidence was observed. Assuming that an inversion suppresses vertical exchange, (1) can be applied separately to the upvalley wind layer and to the layer above. Owing to westerly winds in the upvalley wind layer, (1) is reduced to

$$\frac{\partial \Theta}{\partial t} = -u\,\frac{\partial \Theta}{\partial x} - \frac{1}{\rho c_p}\frac{\partial H}{\partial z}\,. \qquad (2)$$

Table 1. Spatial Mean SF_6 Concentrations at the Cross Sections of Krappel (KA), Marxenhof (MA), Kohlengrund (KG), and Values for the Different Monitoring Sites in the Großes Tal (Sites 2 to 10), Schauinsland (SL) (Site 14), and on the Mountain Ridge at Rappeneck (Site 15) on June 5, 1996

Time, CET	KA				MA				KG				SL	RE
	Mean	2	3	4	Mean	5	6	7	Mean	8	9	10	14	15
0900–0930	246	160	268	310	0	0	0	0	0	···	0	···	···	0
0930–1000	942	869	878	1078	0	0	0	0	0	···	0	···	···	0
1000–1030	535	582	473	552	23	17	28	23	24	···	24	0	···	0
1030–1100	290	247	277	347	144	77	162	193	103	81	124	···	36	2
1100–1130	40	15	71	34	110	81	122	128	94	93	114	76	106	35
1130–1200	15	10	24	10	28	16	34	33	31	24	28	41	56	34
1200–1230	···	···	···	···	···	···	···	···	13	11	15	14	21	10
1230–1300	···	···	···	···	···	···	···	···	7	7	6	7	9	6
1300–1330	···	···	···	···	···	···	···	···	5	5	5	6	6	5

Concentrations are in parts per trillion. No entry indicates no measurements are available.

The divergence of $H(z)$ can be calculated from the value at the surface, H_0, and at the top of the mixed layer, $H(z_i)$. $H(z_t)$ generally ranges from $H(z_t) \approx 0$ to $H(z_t) \approx -0.2\, H_0$ [*Stull*, 1988]. At 0900 CET, $H_0 \approx 100$ W m^{-2} (Figure 8), and z_t = 170 m; heating of the mixed layer by the divergence of the sensible heat flux was approximately 1.5 K h^{-1}. However, between 0720 and 0906 CET the local heating observed in this layer was only 0.25 K h^{-1} (Figure 8). So horizontal advection of cold air from the Rhine Valley must be responsible for the fact that nearly no temperature increase was observed between 0720 and 0906 CET.

As the sensible heat flux of the layer between the first inversion at 170 m above ground level (agl) and the second inversion at 1400 m msl at 0900 CET is approximately zero, the divergence of the sensible heat flux can be neglected. Thus the budget equation (1) is reduced to

$$\frac{\partial \Theta}{\partial t} = -u\,\frac{\partial \Theta}{\partial x} - v\,\frac{\partial \Theta}{\partial y}; \tag{3}$$

that is, the local heating of 0.7 K h^{-1} observed between 0720 and 0906 CET (Figure 8) must result from a horizontal advection of warm air. To prove this assumption, the temperature profiles from the Zarten Basin were compared with those of elevated areas of the Black Forest hills (Figure 8). While the temperature profiles at Ebnet and Oberried in the Bruggatal between 600 m msl and 1000 m msl were similar at 0700 CET, the temperature over the mountainous sites (BT, GT) was already about 1 K higher at 0900 CET than that of the air over the basin. Assuming southeasterly winds at approximately 3 m s^{-1} (Figure 7) and the temperature gradient of 1 K between Ebnet and the mountain sites 12 km in the southeast results in a heating of 0.9 K h^{-1}. This is in agreement with the local

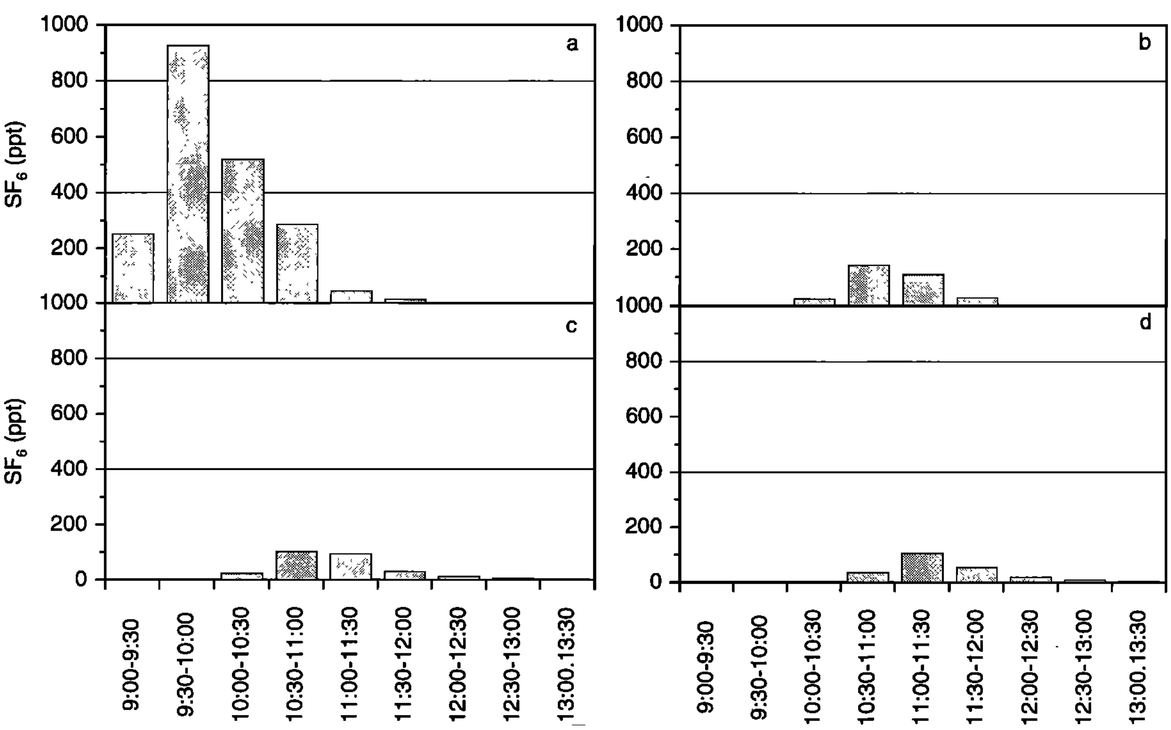

Figure 9. Mean SF_6 concentrations in the Großes Tal at (a) Kappel, (b) Marxenhof, (c) Kohlengrund, and (d) Schauinsland on June 5, 1996. The positions of the different sites are indicated in Figure 1.

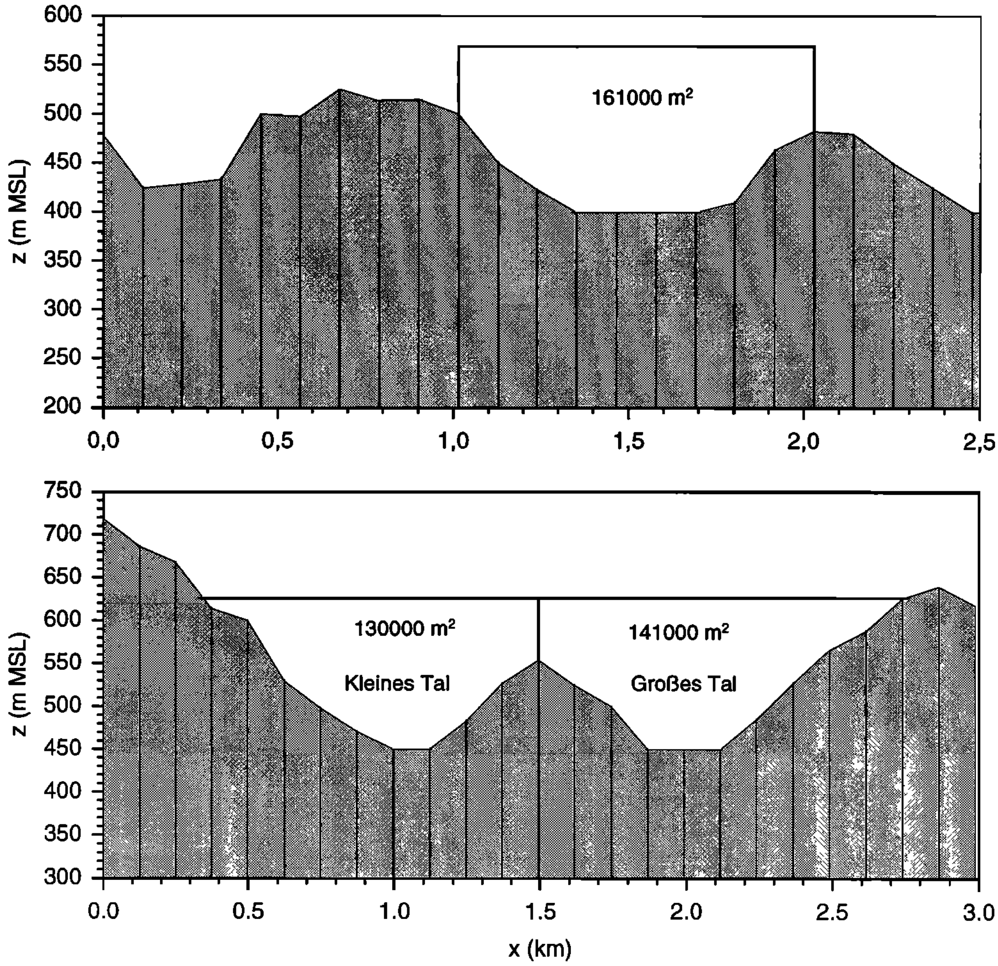

Figure 10. Cross-section areas normal to the valley axis of the Großes Tal at the positions of (top) Kappel and (bottom) Maierhof. The positions are indicated in Figure 1.

heating rate observed of 0.7 K h^{-1} in this layer at 0900 CET (Figure 8). It may therefore be concluded that cold air advection in the upvalley regime and warm air advection above results in the maintenance of the low-level inversion and suppressed mixed-layer growth in the Zarten Basin. A similar phenomenon, that is, the formation of an elevated mixed layer (EML) over the mountains, which then is horizontally advected to the surrounding lower terrain, has been observed and described by *Arritt et al.* [1992] for an area in the lee of the Rocky Mountains over eastern Colorado. *Kuwagata et al.* [1995] observed such a phenomenon as well.

4. Transport and Dispersion of SF_6

4.1. Tracer Experiment

In order to investigate the contribution of dispersion to the change of the concentration of air pollutants on their way from the entrance of the Großes Tal to the outlet, SF_6 was released simultaneously from three sites in the Zarten Basin between 0900 and 1030 CET (Figure 1). At this time the valley wind in the Zarten Basin had already developed, and the surface layer is unstably stratified (Figure 5) so that mixing of the tracer up to the inversion (section 3.2.2) can be assumed. A background concentration of 4.5 ppt was found for the area and subtracted from the observations. Table 1 summarizes the mean concentrations at the three cross sections at Kappel (sites 2, 3, 4), Marxenhof (sites 5, 6, 7), Kohlengrund (sites 8, 9, 10), as well as the measurements at the monitoring sites (sites 2 to 14) in the Großes Tal and on the ridgetop at Rappeneck (site 15). Figure 9 contains the mean concentrations at the three cross sections and at Schauinsland. At Kappel the mean SF_6 concentration was 250 ppt between 0900 and 0930 CET. At this site the peak of 942 ppt appeared between 0930 and 1000 CET. Afterward, the concentration decreased again, and only 15 ppt were found between 1130 and 1200 CET. At Marxenhof the first tracer concentrations were detected between 1000 and 1030 CET, and a peak of 144 ppt appeared between 1030 and 1100 CET. This means that the peak concentration had dropped to $\frac{1}{6}$ between Kappel and Marxenhof, a distance of 3.4 km only. At Kohlengrund the SF_6 peak of 103 ppt arrived between 1030 and 1100 CET, that is, in the same time intervals as at Marxenhof 1.2 km upstream. Finally, at Schauinsland the SF_6 peak of 105 ppt was detected between 1100 and 1130 CET.

Analysis of the data from each of the monitoring sites shows that concentrations at the different cross sections are not homogeneously distributed. Especially in the first half of the Großes Tal (Kappel (sites 2, 3, 4), Marxenhof (sites 5, 6, 7)), mostly higher concentrations can be found on the eastern slopes of the valley than on the western slopes (Table 1). The Rappeneck station (site 15) just below the mountain ridge (Figure 1) experienced the first tracer between 1030 and 1100

Table 2. Mixed-Layer Depth z_i at Ebnet (EB), Kappel (KA), Molzhof (MO), Kohlengrund (KG), and Oberried (OR)

Time, CET	EB	KA	MO	KG	OR
0830	170	115	...	240	125
1030	190	225	230	308	250
1200	373	445	405	385	250
1330	473	535	695	453	375

Depth is in meters above ground level.

CET, with a peak level of 35 ppt between 1100 and 1130 CET. The reason for the inhomogeneous distribution can be found from the model calculations which show that the flow has a strong northwesterly component when entering the Großes Tal and moving up the easterly slopes [*Fiedler et al.*, this issue]. So at the different cross sections additional monitoring sites up to the mountain ridges would have been of advantage and should be considered for future studies.

To sum up, the measurements of tracer transport in the Großes Tal indicate the following: (1) There was a transport time of 90 ± 5 min between Kappel at the entrance and Schauinsland at the outlet of the Großes Tal; (2) As the distance between both sites is 6.8 km, the propagation rate was approximately 1.3 m s^{-1}. This is slightly below the mean surface wind which was approximately 1.8 m s^{-1} for the Großes Tal during the period between 0900 and 1300 CET. (3) In the propagation from the entrance of the valley to Schauinsland, the peak of the tracer concentration decreased from 942 to 105 ppt, which gives a dilution factor of approximately 9.

4.2. Tracer Dilution Caused by Mixed Layer Growth

The concentration C of a tracer is supposed to decrease with the increase in the cross section A, over which the tracer is mixed. The ratio of the tracer concentrations, C_1/C_2, at sites 1 and 2 should be inversely correlated to the ratio of the cross sections, A_2/A_1, at the corresponding sites,

$$\frac{A_1}{A_2} = \frac{C_2}{C_1} \tag{4}$$

Assuming that the tracer is mixed over the entire depth of the valley wind, A defines the area between the valley ground and the mixed-layer top. In addition to the increase in the mixed layer, the concentration may be reduced by venting of the tracer through the upslope winds out of the valley into the free atmosphere, A_{slope}. The reduction in tracer concentration by upslope winds depends on the strength of the slope wind, v_{slope}, the time t it takes to pass from cross section A_1 to cross section A_2, and the height of the upslope wind regime, h_{slope}:

$$A_{\text{slope}} = v_{\text{slope}}\, t\, h_{\text{slope}}. \tag{5}$$

Thus the concentration C_2 at site A_2 is given by

$$C_2 = C_1 \times \frac{A_1}{(A_2 + A_{\text{slope}})}. \tag{6}$$

Owing to the lack of data for the upslope winds, the decrease of the tracer concentration is only calculated from mixed-layer growth. Figure 10 shows the cross section normal to the axis of the valley at the two sites of Kappel (KA) and Maierhof (MH). The mixed-layer depths at the different sites, necessary for the application of (6), are summarized in Table 2. At Kappel, between 0930 and 1000 CET, the tracer was assumed to be mixed over an area of about A_1 = 161,000 m^2 (z_i = 180 m). On the way south, at Maierhof, the valley splits into two valleys, Großes Tal and Kleines Tal (Figure 1). It is therefore assumed that the tracer moves into both valleys and is diluted over the total of A_2 = 271,000 m^2 (z_i = 180 m). This results in a decrease of concentration to C_2 = 559 ppt. In the Großes Tal, from Maierhof to Marxenhof, the tracer then moves on at this concentration level. The corresponding cross section of the Großes Tal at Maierhof is $A_{2,G}$ = 141,000 m^2 (Figure 10), increasing to A_3 = 329,000 m^2 at Marxenhof (z_i = 285 m). This results in a tracer concentration of C_3 = 240 ppt. At Kohlengrund a mixed layer depth of z_i = 350 m at 1100 CET gives a cross section of A_4 = 315,000 m^2 and a corresponding tracer concentration of 250 ppt. The concentrations at Marxenhof and Kohlengrund are higher than the measured mean concentrations of 144 ppt at Marxenhof and 103 ppt at Kohlengrund. Thus it can be concluded that the decrease of the tracer cannot only be explained by the mixed-layer growth. The model simulations performed by *Fiedler et al.* [this issue] indicate that the decrease of the tracer concentration results in three processes: mixing layer growth, flow splitting, and mountain venting.

5. Conclusions

In June 1996 the Schauinsland Ozone Precursor Experiment (SLOPE) was conducted to investigate the evolution, as a function of time, of ozone and its precursors between Freiburg in the Rhine Valley and Schauinsland in the Black Forest. This study was conducted to calculate the contribution of dispersion to the dilution of trace gases in a propagating air mass. This was done by releasing the inert tracer SF_6 and performing comprehensive meteorological measurements using surface stations, sodars, tethersondes, and radiosondes. The latter systems furnished information about the valley wind regime and the evolution of the mixed layer. These are the main results of the experiment:

1. Clear-sky conditions caused upvalley winds to be generated in the valleys in the morning. The onset of the upvalley wind in the smaller Großes Tal at 0730 CET was approximately 1.5 hours earlier than in the longer and broader Zarten Basin (0900 CET). Nevertheless, upvalley winds existed in the valleys when the tracer release started at 0900 CET in the Zarten Basin.
2. The depth of the upvalley wind regime corresponded to the mixed-layer depths in the valleys.
3. Around midday, the upvalley wind regime was disturbed by regional-scale westerly winds which were observed at elevated stations (Schauinsland, Rappeneck). This time restricts the period for the calculation of the dilution factor because after midday the transport path for air pollutants which arrive at Schauinsland is totally different from that during the morning hours.
4. Transport of the tracer through the Großes Tal took 90 ± 5 min, which yields a propagation of approximately 1.3 m s^{-1}.
5. The dilution factor for the tracer between the entrance of the Großes Tal at Kappel and the outlet at Schauinsland was approximately 9. The decrease of the tracer cannot only be explained by the mixing layer growth.

The results obtained from these investigations were used, together with the model calculations [*Fiedler et al.*, this issue], to calculate the chemical transformation rates for the ozone precursors between the entrance and the outlet of the Großes Tal [*Volz-Thomas and Kolahgar*, this issue].

Acknowledgments. The authors would like to thank all groups involved in the SLOPE experiment, especially the Universities of Paderborn, Freiburg, Stuttgart, Cologne, and GKSS Geesthacht. Some measurements were supported by the Baden-Württemberg State Ministry for Science and Research under contract 1499Tit.Gr.74 within the framework of the Regio-Klima-Project (REKLIP).

References

Allwine, K. J., Atmospheric dispersion and tracer ventilation in a deep mountain valley, *J. Appl. Meteorol.*, *32*, 1017–1037, 1993.

Arritt, R. W., J. M. Wilczak, and G. S. Young, Observations and numerical modeling of an elevated mixed layer, *Mon. Weather Rev.*, *120*, 2869–2880, 1992.

Atkinson, B. W., *Meso-Scale Atmospheric Circulations*, 495 pp., Academic, San Diego, Calif., 1981.

Barry, R. G., *Mountain Weather and Climate*, 402 pp., Routledge and Kegan Paul, New York, 1992.

Bischoff-Gauß, I., N. Kalthoff, and F. Fiedler, The impact of secondary flow systems on air pollution in the area of Sao Paulo, *J. Appl. Meteorol.*, *37*, 269–287, 1998.

Carroll, J. J., and R. L. Baskett, Dependence of air quality in a remote location on local and mesoscale transports: A case study, *J. Appl. Meteorol.*, *18*, 474–486, 1979.

Clements, W. E., J. A. Archuleta, and P. H. Gudiksen, Experimental design of the 1984 ASCOT field study, *J. Appl. Meteorol.*, *28*, 405–413, 1989.

de Wekker, S. F. J., The behavior of the convective boundary layer height over orographically complex terrain, diplomarbeit, Dep. of Meteorol., Wageningen Agric. Univ. and Meteorol. Inst. Univ. Karlsruhe, Karlsruhe, Germany, 1995.

Fiedler, F., I. Bischoff-Gauß, N. Kalthoff, and G. Adrian, Modeling of the transport and diffusion of a tracer in the Freiburg-Schauinsland area, *J Geophys. Res.*, this issue.

Freytag, C., Results from the MERKUR experiment: Mass budget and vertical motions in a large valley during mountain and valley wind, *Meteorol. Atmos Phys.*, *37*, 129–140, 1987.

Freytag, C., Atmospharische Grenzschicht in einem Gebirgstal bei Berg- und Talwind, *Wiss. Mitt. 60*, 197 pp., Meteorol. Inst., Univ. Munchen, Munchen, Germany, 1988.

Groß, G., Numerical simulation of the nocturnal flow systems in the Freiburg area for different topographies, *Contrib. Phys. Atmos.*, *62*, 57–72, 1989.

Gudiksen, P. H., G. J. Ferber, M. M. Fowler, W. L. Eberhard, M. A. Fosberg, and W. R. Knuth, Field studies of transport and dispersion of atmospheric tracers in nocturnal drainage flows, *Atmos. Environ.*, *18*, 713–731, 1984.

Hennemuth, B., Thermal asymmetry and cross-valley circulation in a small Alpine valley, *Boundary Layer Meteorol.*, *36*, 371–394, 1986.

Kalthoff, N., H.-J. Binder, M. Koßmann, R. Vogtlin, U. Corsmeier, F. Fiedler, and H. Schlager, Temporal evolution and spatial variation of the boundary layer over complex terrain, *Atmos. Environ.*, *32*, 1179–1194, 1998.

King, J. A., F. H. Shair, and D. D. Reible, The influence of atmospheric stability on pollutant transport by slope winds, *Atmos. Environ.*, *21*, 53–59, 1987.

Koßmann, M., R. Vögtlin, U. Corsmeier, B. Vogel, F. Fiedler, H.-J. Binder, and N. Kalthoff, Aspects of the convective boundary layer structure over complex terrain, *Atmos. Environ.*, *32*, 1323–1348, 1998.

Kraus, H., Die Energieumsätze in der bodennahen Atmosphäre, *Ber. Dtsch. Wetterdienstes. 117*, 43 pp., Dtsch. Wetterdienst, Offenbach, Germany, 1970.

Kurita, H., H. Ueda, and S. Mitsumoto, Combination of local wind systems under gradient wind conditions and its contribution to the long-range transport of air pollutants, *J. Appl. Meteorol.*, *29*, 331–348, 1990.

Kuwagata, T., and F. Kimura, Daytime boundary layer evolution in a deep valley, part I, Observations in the Ina valley, *J. Appl. Meteorol.*, *34*, 1082–1091, 1995.

Loßnitzer, H., Einige Bemerkungen zum Klima Freiburgs im Breisgau. *Z. Angew. Meteorol. "Wetter," 59*, 37–42, 1942.

Möllmann-Coers, M., and K. Heinemann, Verwendung von SF_6 bei der Untersuchung der Schadstoffausbreitung und -transport in der Atmosphäre im Forschungszentrum Jülich, *ASS-Ber. 0652*, 12 pp., Abt. Sicherheit und Strahlenschutz, Jülich, Germany, 1997.

Neininger, B., Flugzeugmessungen fur SLOPE-96 5. bis 28. Juni, 1996, internal report, 1996.

Orgill, M. M., Early morning ventilation of a gaseous tracer from a mountain valley, *J. Appl. Meteorol.*, *28*, 636–651, 1989.

Pätz, H.-W., et al., Measurements of trace gases and photolysis frequencies during SLOPE96 and a course estimate of the local OH concentration from HNO_3 formation, *J. Geophys. Res.*, this issue.

Rudloff, H., Besonderheiten im Klima von Freiburg, *Bad. Landesver. f. Naturschutz*, *NF* 5, 237–254, 1980.

Segal, M., C.-H. Yu, R. W. Arritt, and R. A. Pielke, On the impact of valley/ridge thermally induced circulations on regional pollutant transport, *Atmos. Environ.*, *22*, 471–486, 1988.

Steinacker, R., Area-height distribution of a valley and its relation to the valley wind, *Contrib. Atmos. Phys.*, *57*, 64–71, 1984.

Stull, R. B., *An Introduction to Boundary Layer Meteorology*, 666 pp., Kluwer Acad., Norwell, Mass., 1988.

Vergeiner, I., and E. Dreiseitl, Valley winds and slope winds—Observations and elementary thoughts, *Meteorol. Atmos. Phys.*, *36*, 264–286, 1987.

Vögtlin, R., M. Koßmann, H. Güsten, G. Heinrich, F. Fiedler, U. Corsmeier, and N. Kalthoff, Transport of trace gases from the upper Rhine Valley to a mountain site in the northern Black Forest, *Phys. Chem. Earth*, *21*, 425–428, 1997.

Volz-Thomas, A., and B. Kolahgar, On the budget of hydroxyl radicals at Schauinsland during SLOPE, *J. Geophys. Res.*, this issue.

Volz-Thomas, A., H. Geiß, and N. Kalthoff, Schauinsland Ozone Precursor Experiment (SLOPE96): Scientific background and main results, *J. Geophys. Res.*, this issue.

Wakimoto, R. M., and J. L. McElroy, Lidar observation of elevated pollution layers over Los Angeles, *J. Clim. Appl. Meteorol.*, *25*, 1583–1599, 1986.

Whiteman, C. D., Morning transition tracer experiment in a deep narrow valley, *J. Appl. Meteorol.*, *28*, 626–635, 1989.

Whiteman, C. D., Observations of thermally developed wind systems in mountainous terrain, in *Atmospheric Processes Over Complex Terrain*, *Meteorol. Monogr.*, vol. 23, edited by W. Blumen, pp. 5–42, Am. Meteorol. Soc., Boston, Mass., 1990.

Wilson, R., F. Shair, B. Reynolds, and W. Greene, Characterization of the transport and dispersion of pollutants in a narrow mountain valley region by means of an atmospheric tracer, *Atmos. Environ.*, *17*, 1633–1647, 1983.

Ye, Z., M. Segal, and R. A. Pielke, Effects of atmospheric thermal stability and slope steepness of daytime thermally induced upslope flow, *J. Atmos. Sci.*, *44*, 3341–3354, 1987.

U. Corsmeier, V. Horlacher, and N. Kalthoff (corresponding author), Institut für Meteorologie und Klimaforschung, Forschungszentrum Karlsruhe/Universität Karlsruhe, Postfach 3640, D-76021 Karlsruhe, Germany. (norbert.kalthoff@imk.fzk.de)

H. Geiß, B. Kolahgar, and A. Volz-Thomas, Institut für Chemie der belasteten Atmosphäre, Forschungszentrum Jülich, Julich, Germany.

A. Knaps and M. Mollmann-Coers, Abteilung Sicherheit und Strahlenschutz, Forschungszentrum Jülich, Jülich, Germany.

(Received April 12, 1999; revised September 15, 1999; accepted September 22, 1999.)